Cold Regions Science and Technology 177 (2020) 103113

Contents lists available at ScienceDirect

Cold Regions Science and Technology

journal homepage: www.elsevier.com/locate/coldregions

A low resource subglacial bedrock sampler: The percussive rapid access isotope drill (P-RAID)

Ryan Timoney[a], Kevin Worrall[a], David Firstbrook[a], Patrick Harkness[a,*], Julius Rix[b], Daniel Ashurst[b], Robert Mulvaney[b], Michael J. Bentley[c]

[a] School of Engineering, University of Glasgow, Glasgow G12 8QQ, UK
[b] British Antarctic Survey, Madingley Road, Cambridge CB3 0ET, UK
[c] Department of Geography, Durham University, Durham DH1 3LE, UK

ARTICLE INFO

Keywords:
Polar Drilling
Planetary Drilling
Paleoclimatology

ABSTRACT

The paleoclimate community has an interest in distributed subglacial bedrock sampling but, while capable drill systems do exist, they are often incompatible with Twin Otter logistics aircraft. To address this issue, a design built on the existing low footprint ice-sampler, the Rapid Access Isotope Drill (RAID), is investigated. The new device will retain key features of the parent system, but the ice drilling elements of the RAID will be replaced by a self-contained rotary-percussive core-drill capable of penetrating ice-consolidated and rocky terrain at and below the ice/rock interface. This new front-end will only be deployed once the interface itself has been attained, providing a pristine core sample from the underlying terrain. The proposed Percussive Rapid Access Isotope Drill (P-RAID) has been inspired by planetary drilling technologies to allow autonomous operations at the bottom of the hole. This paper details the development and testing of the proof-of-concept hardware. The mechanical and electrical design challenges encountered, and the results obtained from a series of prolonged cold chamber tests will be discussed, alongside lessons learned from initial testing in Antarctica.

1. Introduction

Almost all of Antarctica, and around 80% of Greenland, is covered by ice, which means that geological science in these regions has mostly been limited to the exploration of isolated nunataks, as well as air- or space-borne geophysical survey. The acquisition of distributed subglacial bedrock samples is therefore an attractive proposition for glaciologists and paleoclimatologists (Clow and Koci, 2002; Flowerdew et al., 2012; Spector et al., 2018), because such samples could enable cosmogenic dating of the surface exposure history. Taken across the continent, these samples could be used to inform about the thickness and extent of the ice sheet over geological time (Clow and Koci, 2002; Sugden et al., 2012).

This is important because the last time CO_2 reached current concentrations (> 400 ppm) the entire West Antarctic Ice Sheet (WAIS) may have been unsustainable, and there is consistent evidence that the sea level was higher during these previous interglacials (Dutton et al., 2015). However, the specific glaciation which contributed to the sea level rise is poorly understood, which creates uncertainty in the relationship between atmospheric (CO_2), glaciological (ice volume), and geographical (sea level) trends.

This uncertainty was deemed to be of critical importance by the recent Intergovernmental Panel on Climate Change (IPCC) fifth assessment (Church, 2013). These types of considerations led the International Partnerships in Ice Core Sciences (IPICS) drillers' meeting to identify “sampling bedrock at the bottom of the hole” to be one of the key challenges in their Ice Core Drilling Technical Challenges White Paper (IPICS, 2020). Looking forwards still further, the development of lightweight wireline drilling technologies may prove to be an essential step in the exploration of Antarctic or even Martian subglacial lakes (Orosei et al., 2018).

2. Challenges of subglacial bedrock sampling

2.1. Logistical drivers

Polar drilling campaigns are complicated by extreme isolation. The development of new technologies should be approached holistically, recognising logistics as a solution driver.

The de Havilland Twin Otter aircraft can transport four scientific personnel and up to one tonne of cargo at any one time, although the internal cargo volume may limit the use of lengthy or bulky hardware.

* Corresponding author.
E-mail address: patrick.harkness@glasgow.ac.uk (P. Harkness).

https://doi.org/10.1016/j.coldregions.2020.103113
Received 27 August 2019; Received in revised form 10 February 2020; Accepted 1 June 2020
Available online 03 June 2020

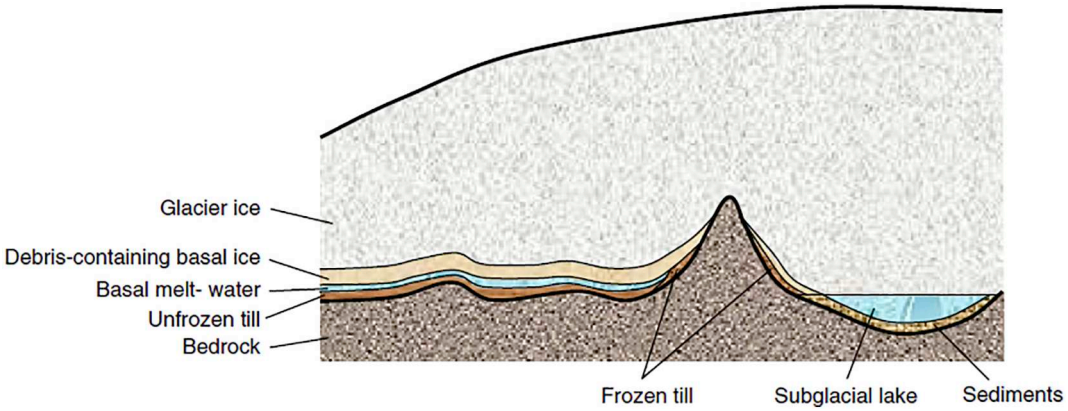

Fig. 1. Schematic of subglacial layering (Talalay, 2013).

Aircraft are also often highly committed during the polar summer months, and operate near the edge of their range and performance envelopes.

Therefore, to ensure that any sampling system can be deployed to the most interesting field locations, the architecture should be compatible with aircraft of this size and payload capacity (Triest et al., 2014). Ideally, all the (disassembled) components should be delivered on a single sortie, along with the petroleum and generators required for the entire duration of the campaign.

2.2. Technical drivers

A highly-deployable subglacial bedrock sampler must extract cores from a variety of terrains and, as shown in Fig. 1, the working environment may consist of debris-rich basal ice, a melt layer, till material, and bedrock (Talalay, 2013). The bedrock may be sedimentary, metamorphic, or igneous, and given the glaciation above, there will be a large amount of erratic material as well.

The drill response will therefore be unpredictable. Harder rocks may be the most difficult to penetrate, but softer rocks with a greater initial rate-of-progress may ultimately increase the failure rate of the drill process through auger choke or other failure modes. The control system must therefore evaluate the progress of the system in real-time, adjusting the drill parameters (such as weight-on-bit, hammer frequency, and auger rpm) in response to mechanical signals such as rate-of-progress and auger torque, as well as (if appropriate) downhole melt conditions indicated by signals such as temperature and electrical conductivity.

The variable topography (National Reseach Council, 2011) of subglacial Antarctica adds another set of constraints for the sampling technology. While previous BAS ice-core drilling operations at Berkner Island (Mulvaney et al., 2014a), James Ross Island, and the Fletcher Promontory (Mulvaney et al., 2014b) have reached bedrock at 948 m, 363 m, and 654 m respectively, the continental ice sheet extends to depths of 4897 m in the Astrolabe Basin (Fretwell et al., 2013).

Only a wireline system, where the drill system is deployed by a spooled tether rather than a series of pipes, combines moderate logistics with applicability across this wide range of ice/rock interface depths. Alternative heavy systems (Goodge and Severinghaus, 2016; IDDO, 2015) are too logistically intensive to deploy widely, which tends to confirm the choice of the RAID architecture as the starting point for the design presented.

3. BAS rapid access isotope drill (RAID)

The RAID is a wireline drill designed to capture ice cuttings from depths up to 600 m, but which trades high-resolution coring for mechanical simplicity. Inspired primarily by the BAS medium-depth ice corer (Mulvaney et al., 2002), the drill system acquires multi-metre 'pecks' from the icepack by means of an upper anti-torque stage (sprung skegs or skates against the borehole walls) which reacts against a rotating casing in the lower section. The cuttings are drawn into the casing and climb a central, stationary auger until the peck depth is reached. The drill system is then winched to the surface where the casing is reversed to expel the cuttings for isotopic analysis. The drill cycle is then repeated. The device uses a single, Maxon brushless DC motor with a power requirement of less than 1 kW downhole, and employs commercial electronics both downhole and at the surface. The winch assembly can place the drill system to the bottom of the hole, and raise it back to the surface, with an accuracy of a few cm.

The RAID can reach its maximum depth in approximately one week of cyclic operations, but it is unable to sample subglacial bedrock because the cutters are optimised for planing ice rather than breaking rock, as shown in Fig. 2. The ground system consists of a winch and a control unit, with the winch assembly designed to be setup in the field. The mast comes in two parts for ease of transportation, as shown in Fig. 3.

The RAID therefore provides an excellent baseline for the new subglacial bedrock sampler. The lower rotating barrel and central auger will be removed from the drill system and replaced with the proposed rock sampler for the final drill cycle. However, the winch will be retained, as will the upper anti-torque stage of the drill system so that downhole auger loads might be reacted. The retained upper drill system works will also provide inertia, to deliver rock-breaking percussion forwards into the bedrock, and create weight-on-bit more generally. Overall, RAID heritage should provide a more mature concept from the very first iteration (Rix et al., 2019).

4. Drill design considerations

4.1. Analogies in planetary exploration

Subglacial bedrock sampling shares many of the challenges associated with the exploration of the terrestrial planets. Weight-on-bit, torque, power, mass, and dimensions are at a premium, the downhole conditions are diverse and relatively unknown, there is a risk of freeze-in, and autonomous control of local operations is required to ensure consistent progress and to quickly respond to any developing failure modes.

4.2. Rock penetration

Rotary drilling uses a combination of weight-on-bit and rotation to fracture the rock through compression and shear. Eq. (1) demonstrates that the power required to operate such a system, P_{pe}, arises from two elements (Zacny et al., 2008a), namely the torque, T, required to

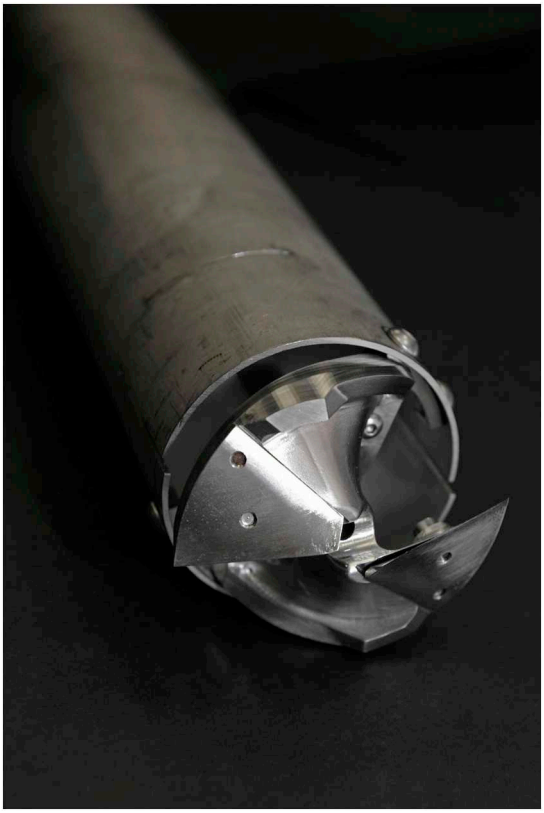

Fig. 2. RAID front end, with the ice cutters and rotary barrel visible. The system diameter is 80 mm.

overcome drilling friction, P_{fri} (Eq. (2)), and the effort required to fracture the terrain, P_{fra} (Eq. (3)). In the equations w is weight-on-bit, r is the radius of the drillbit, μ is the friction coefficient, and ω is the angular rate.

The energy required to fracture the terrain at a given volumetric rate of progress is directly proportional to the uniaxial compressive strength of the rock, σ, so a robust system must deliver sufficient weight-on-bit to overcome this effect. The system must also provide enough torque to overcome the frictional forces generated by the weight-on-bit, with this torque being delivered at an rpm that can support augering for spoil extraction. As indicated above, this process will generate a further auger torque.

$$P_{pe} = P_{fri} + P_{fra} \tag{1}$$

$$P_{fri} = T\omega = wr\mu\omega \tag{2}$$

$$P_{fra} = \sigma r^2 \delta\omega/2 \tag{3}$$

Rotary drill systems designed to operate with reduced drilling forces and torques may still require 3 kN to 5 kN of weight-on-bit, with corresponding torque of up to 50 Nm and power requirements in the region of 3 kW, in igneous and metamorphic formations (Cao et al., 2014). While such systems may be classified as low-resource compared to industrial rigs, it is unlikely that our P-RAID will be able to operate at this level. A modified approach will therefore be required.

Percussive drilling, where a repeated hammering load is applied to the drillbit, may be a viable alternative to conventional rotary drilling in low resource settings (Talalay, 2013; Wang et al., 2015). In fact, it has been demonstrated that rotary-percussive drilling may be seven times faster than rotary drilling in hard formations (Melamed et al., 2000).

Despite much discussion (Samuel, 1996) we are unaware of any published attempts to incorporate a percussive actuator into a wireline drill system, perhaps because terrestrial rigs do not require downhole

Fig. 3. The RAID winch system on the surface. The disassembled tower can be transported in a single Twin Otter sortie.

percussion when high forces and torques are available at the surface. However, there are three common percussive mechanisms in planetary drill concepts which may be applicable here:

1) Spring-cam actuated hammer mechanism
2) Voice-coil actuated hammer mechanism
3) Ultrasonic-percussive hammer mechanism

The spring-cam has been used in various drilling concepts and systems for the Moon and Mars (Chu et al., 2014; Zacny et al., 2013; Quan et al., 2012). The principle usually involves the rotation of a spring loaded cam-follower/hammer assembly within a static,

circumferential barrel cam profile, although the stator and rotor parts can be reversed. The cam profile causes the spring to be compressed until the next cam drop is reached, when the cam-follower/hammer is propelled downwards and into the anvil at the top of the drillbit. A stress wave propagates into the terrain, causing fractures which may extend far beyond the initial indentation (Han and Dusseault, 2005). Percussive energies of 0.5 J to 5 J per blow are typical, with an overall power of perhaps 15 W to 100 W depending on the size of the motor which can be accommodated in the concept architecture.

The voice-coil uses an electromagnet to retract a hammer, compressing a spring in the process. When the power is cycled, the hammer is propelled towards the anvil as before. The reduced number of moving parts is an advantage, and the efficiency of the system can be high due to an option for energy recovery on the rebound (Okon and NASA Kennedy Space Center, 2010). However, the control electronics required to implement a voice-coil system with chaotic hammering may be complex, because the rebound characteristic will likely vary with every single blow.

The ultrasonic-percussive technique uses an ultrasonic transducer to convert electrical energy into a mechanical output in the form of longitudinal or longitudinal-torsional vibration in a tuned sonotrode, which is then converted again by a free-flying mass oscillating between the sonotrode and the anvil (Bar Cohen et al., 2003). However, high voltage electronics are required to excite the transducer, the ultrasonic stack can be challenging to scale, and motion control is challenging because the oscillation can stall when excessive weight-on-bit is applied.

Percussive drilling, with a spring-cam mechanism, will be selected for development in the P-RAID concept.

4.3. Spoil removal techniques

After the rock has been penetrated, the spoil must be removed. This will create an additional power requirement, but if it is not carried out, progress will stall while the existing cuttings are reground over and over again. In contrast to the rock penetration activity, which is facilitated by softer rocks, spoil extraction is often easier to achieve in harder materials, as these tend to produce fewer cuttings as a function of time.

Augering is a highly effective process by which a rotating drillbit with helical features uses a combination of centrifugal effects, wall friction, and apparently rising flutes to convey the cuttings upwards. The process is highly dependent on both the diameter and rotational speed of the drillbit, and is best suited to dry fines.

Pneumatic clearing uses pressurised gas, delivered to the bottom of the borehole, as a clearing mechanism (Zacny et al., 2005). Efficiency can be high, depending on the pressure differential, and inexpensive gases such as compressed air can be used. However, the delivery of the gas to the bottom of the hole can be challenging, particularly in a wireline system.

Cutting fluids can be circulated to extract spoil, and in subglacial drilling they often play an important role in borehole stabilisation through hydrostatic pressure. However, the use of fluids increases the logistics efforts required, negating the potential advantage of the proposed design. In addition, these fluids are pollutants, and they are typically removed from the environment at the end of the drill cycle if this is at all possible.

Given the lightweight, low resource and environmentally sensitive nature of the development, augering will be selected for development in the P-RAID concept. It is envisaged that any fluid will be extracted immediately before the insertion of the P-RAID, which will operate in essentially dry borehole conditions.

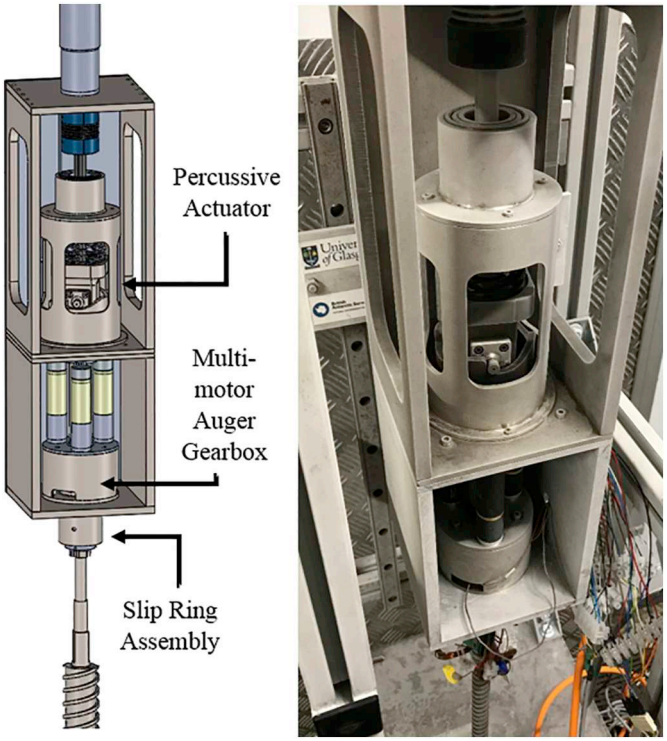

Fig. 4. P-RAID breadboard CAD (left); and the hardware after cold testing (right).

5. P-RAID breadboard

5.1. Architecture

The breadboard has a modular design so that items such as cams, drillbits, and motors can be exchanged for testing and repair. The central footprint of the breadboard also matches the RAID borehole diameter to ensure that the kinematics of the system are representative of future field-ready models. As can be seen in Fig. 4, the breadboard module consists of a percussive actuator assembly, a multi-motor auger gearbox assembly and a slipring assembly. These will be discussed in more detail in Sections 5.2, 5.3, and 5.4 respectively.

5.2. Percussive actuator

Spring-cam percussion can be combined with drillbit rotation using a field-proven spline assembly (Worrall et al., 2018), and cam geometry is a very important element of the overall design. Because it was foreseen that percussive frequencies of up to 20 Hz would be used, the cam could be classified as a “high speed” piece (Norton, 2009) and is thus particularly susceptible to wear. Fig. 5 (Chu et al., 2008) shows how serious this can be, destroying a cam made of 17–4 stainless steel, hardened to H900 condition, within an hour of operation. This is unacceptable.

A cycloidal cam geometry was therefore explored, where the acceleration profile is instead based on a full-period sinusoid. Cam design requires particular attention to the acceleration profile, and an ideal geometry would feature acceleration and jerk profiles which are continuous or, at worst, feature only finite discontinuities.

Eqs. (4), (5), and (6) detail the acceleration, a, velocity, v, and displacement, s, profiles of a cycloidal geometry, where h denotes the maximum follower vertical rise, β denotes the total angle of the segment, and θ is the cam angle.

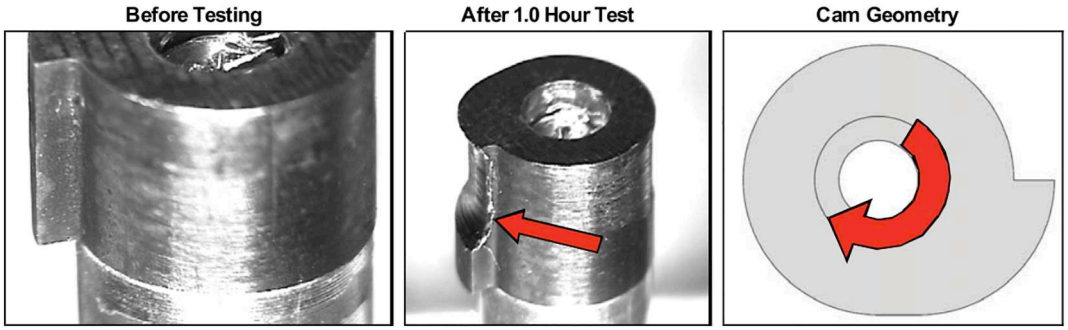

Fig. 5. An example of wear on a poorly designed cam. This damage occurred after one hour of operations at 88 Hz (Chu et al., 2008).

$$a = 2\pi\frac{h}{\beta^2}\,sin\left(2\pi\frac{\theta}{\beta}\right) \tag{4}$$

$$v = \frac{h}{\beta}\left[1 - cos\left(2\pi\frac{\theta}{\beta}\right)\right] \tag{5}$$

$$s = h\left[\frac{\theta}{\beta} - \frac{1}{2\pi}\,sin\left(2\pi\frac{\theta}{\beta}\right)\right] \tag{6}$$

Analysis of the jerk, acceleration, velocity and displacement characteristics of the cycloidal geometry suggests that it is well suited for use as a high-speed barrel cam. The specific design is bounded by key constraints, as follows:

1. The torque required to rotate the cam-follower/hammer around the cam geometry should be deliverable by an off-the-shelf motor with subglacial heritage.
2. The motor must be accommodated within an 80 mm diameter volume, given the diameter of the existing RAID system which will be used create the access bore through the ice.
3. The power demand should not exceed 500 W, or approximately half of the total power supplied from the surface, to ensure compatibility with the existing electrical setup for the RAID.
4. Percussive energies in the region of 1 J to 5 J per blow, and 90 W overall, are indicated by existing cam-hammer systems. This should permit penetration of even hard materials.
5. A cam lifetime of at least 250,000 revolutions, without significant degradation, is indicated by existing cam-hammer systems. This should permit a full-depth (30 cm) cycle without replacement of the cam.

Given that BAS have a long history of using Maxon electronically commutated (EC) brushless DC motors for polar drilling applications, this series is selected for P-RAID. Modifications such as the repackaging of the standard terminal cap of the EC45 and EC60 allows these motors to be accommodated within the restricted borehole constraint, and identification of the motor and gearbox options available allows an upper bound to be set on the deliverable torque.

While an upper bound on the maximum percussive rate of the actuator can be set by the rpm of the gearbox output shaft, the effective maximum is reduced by the cam mechanics. To optimise the delivery of percussion and avoid a collision between the cam-follower/hammer and the ramped section of the cycloidal cam geometry, the quarter-periodicity, $T_{1/4}$, of the system must be found using Eq. (7). In this equation k is the spring stiffness (a wave spring is used to ensure that the force is applied entirely axially) and m is the mass of the cam-follower/hammer assembly.

$$T_{1/4} = \frac{\pi}{2\sqrt{\frac{k}{m}}} \tag{7}$$

The quarter-periodicity indicates the time taken to complete a percussive down stroke, which maps to the period between the cam-follower/hammer rolling over the cam drop and the tip of the hammer engaging with the anvil. This sets the effective maximum rpm because the cam-follower/hammer should not be rotated past the flat, or idle, portion of the cam before the blow has been delivered, because otherwise the cam-follower/hammer rollers would impact against the next incline of the cam. A backstop surface prevents excessive movement of the cam-follower/hammer such that the same impact can never occur, however infrequently, against the low-lying flats of the cam.

Having constrained both the maximum torque deliverable by the motor and the percussive rate which can be achieved, cam geometries may be generated using the equations of cycloidal motion (Quan et al., 2012). To ensure axial loading, and assuming two opposing rollers on the cam-hammer/follower assembly as shown in Fig. 6, only even numbers of cam drops may be used in a practical system.

Each cam geometry can trade-off between blow energy and total power for a given motor and gearbox selection. A reduced number of drops minimises the torque required to rotate the cam-follower/hammer over a given height, but more drops will provide a faster blow rate at a given rpm. The torque itself will be a function of the spring stiffness, and the wave spring (which rotates with the cam-hammer/follower) must be selected according to stiffness, length, and diameter. Fig. 7 details the torque required around 1-drop, 2-drop, and 4-drop cam geometries for a vertical displacement of 17 mm and spring stiffness of 20 kN/m. Fig. 8 shows a relationship between torque and displacement.

An ideal cam design would produce a torque demand closely matching the torque deliverable by motor and gearbox combination, at the desired blow rate.

5.3. Auger and auger gearbox

While the P-RAID uses a hammering action as the primary means of penetrating the target, decoupling the blows from the rotation of the drillbit is essential. Indexing the drillbit with respect to the blows ensures that the full circumference of the drill bit kerf will be impacted in due course, which prevents imprintation of the teeth into the drill site.

Reliance on dry augering for spoil extraction implies a minimum rpm. As indicated in the literature (Zacny and Cooper, 2007), the rotational speed required to convey material through the helical auger, N, is a function of the inclination angle of the helix, i, the radius of the auger, r, the coefficient of friction between the surface of the auger flight and the loose cuttings, μ_s, and the coefficient of friction between the loose cuttings and the surface of the borehole wall, μ_w.

$$N = \frac{30}{\pi}\sqrt{\frac{g}{r}\frac{tan(i) + \mu_s}{\mu_w}} \tag{8}$$

The frictional coefficients between the cuttings and the auger flights, and the cuttings and the borehole wall, are likely to be unknown before deployment. This means that the auger must be designed such that cuttings can be conveyed over a range of downhole frictional

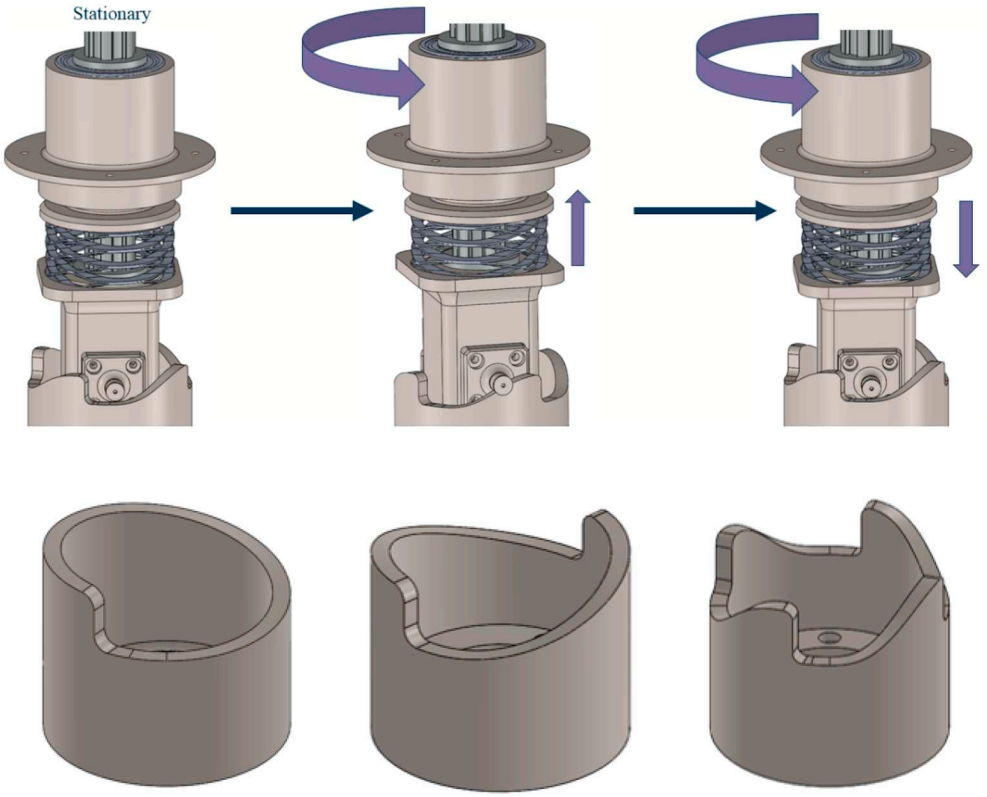

Fig. 6. The operating principle of the cycloidal barrel cam and cam-follower/hammer, showing the rollers and wave spring, along with the spline shaft that allows the cam-follower/hammer assembly to rise and fall with each rotation (above); and 1-drop (not practical), 2-drop, and 4-drop cam geometries which deliver the same blow energy at three different frequencies (below). The cam geometries illustrate the idle periods, the central opening through which the hammer extension passes, and the annular backstop surface which prevents excessive travel of the cam-follower/hammer itself.

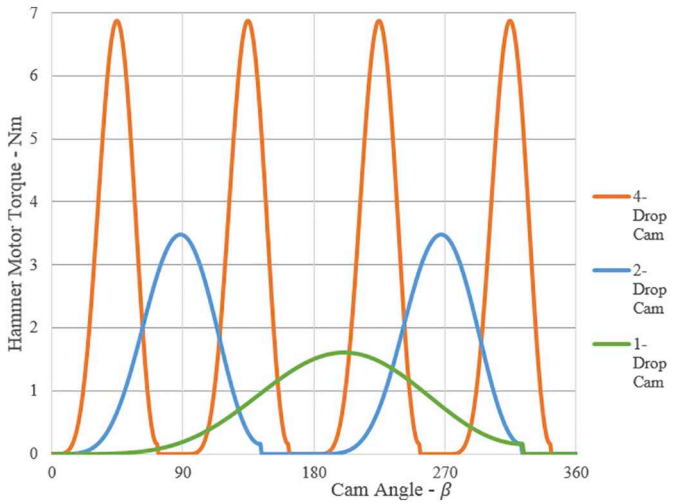

Fig. 7. Hammer motor torque requirements for single, double and quad drop cycloidal barrel cams with a vertical displacement of 17 mm.

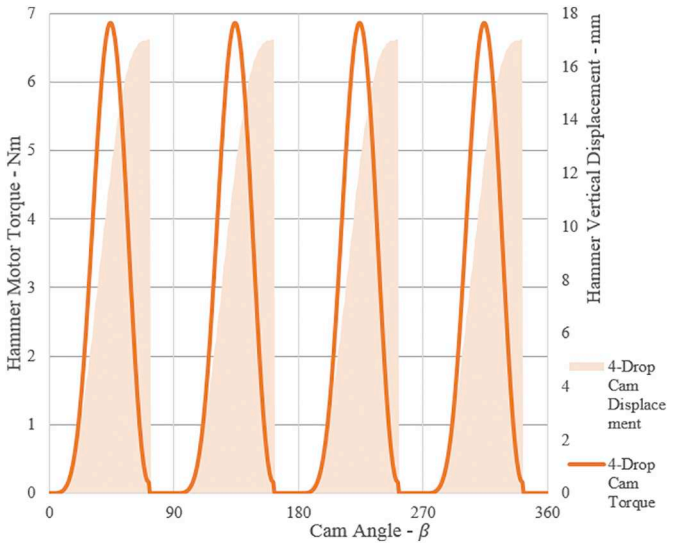

Fig. 8. Torque requirement for 4-drop cam throughout one revolution.

conditions, which drives towards a low helix angle, and creates a tension between minimising radius (and thus minimising the power demanded by Eq. (1)) and maximising radius (and thus minimising the rpm demanded by Eq. (8)). However, for a given coring bit sidewall thickness, the kerf area will increase with the square of the radius and power will scale accordingly. This means that increasing drillbit radius is seldom an effective solution.

When a range of frictional coefficients and drillbit geometries are assumed, speeds in the range of 200 rpm to 300 rpm are indicated. This allows selection of auger motor/gearbox combinations that can deliver downhole torque (Eq. (2)) at a speed which will clear spoil from the bore, with an extra torque reserve to do the work of actually lifting the cuttings.

The diameter constraint makes it difficult to accommodate an appropriate motor/gearbox as a single spur assembly on the central auger drive gear, so teamed motor/gearboxes arranged around the central auger drive gear are required. This provides some redundancy and an increase in torque, but careful control of this setup is required to ensure that the motors to not interfere with one another. The solution is to operate one motor as a master, to control the speed of the assembly during the initial contact with the target, and then increase the torque delivered by the other two motors as the system requires it.

5.4. Slipring and advanced control algorithms

The P-RAID is designed to advance its drillbit at near constant weight-on-bit. The entire breadboard module shown in Fig. 4 runs on

Fig. 9. Examples of melt-and-refreeze faults. Glazing (left); and complete freeze-in (note the use of a chisel to free the piece from the target) (right). Both pieces were drilling in ice-bonded sand at approximately −20 °C.

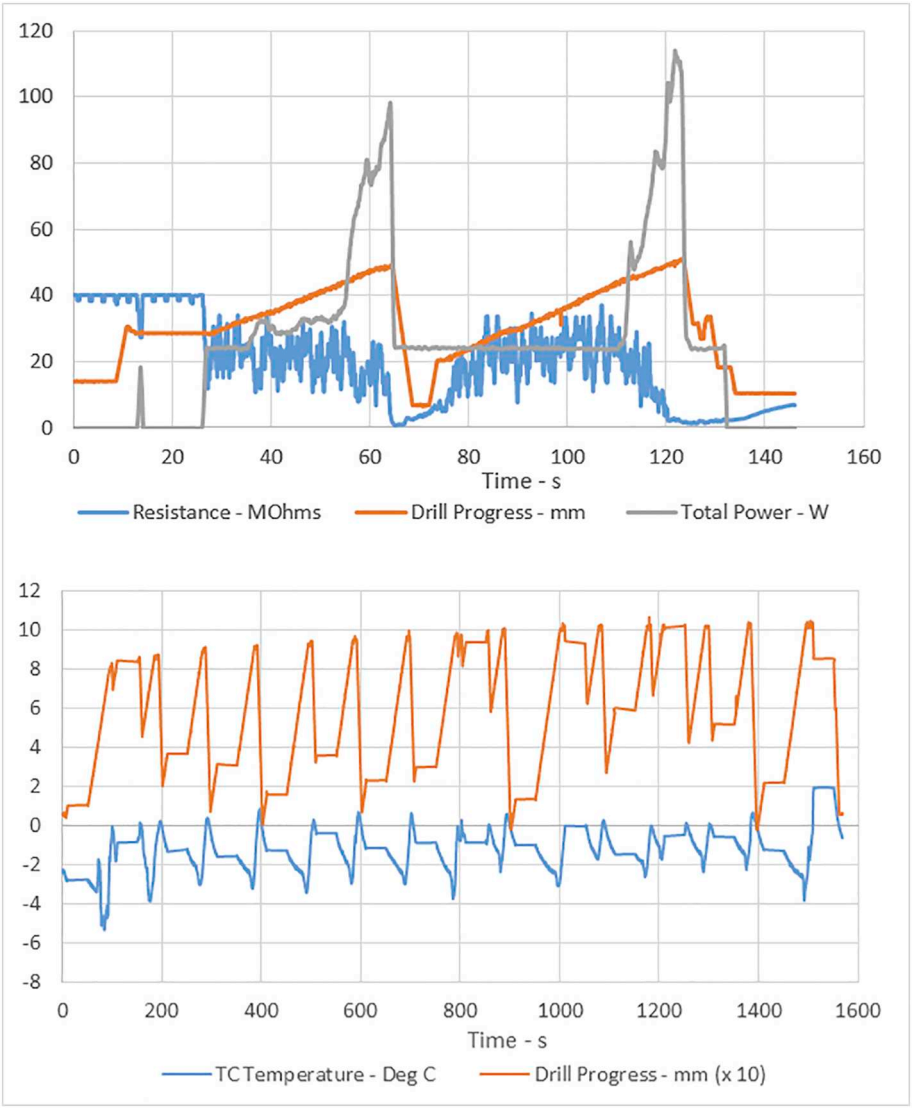

Fig. 10. Experimental drilling runs with drilling governed by electrical resistance feedback (upper panel); and temperature feedback (lower panel). In both cases, the system responds to melt indications by withdrawing the drillbit before a re-freeze process is able to bond the drillbit to the borehole walls. After a short idle period, the drillbit is replaced and drilling continues.

an external guide rail and is positioned by a linear actuator, which is in turn governed by a force transducer. A control loop advances or withdraws the module by a certain progression increment when measured weight-on-bit strays outside a dead zone centred on the target value. This movement has the effect of compressing or relaxing a spring, which floats the auger within the splined core of the central auger drive gear, so the control movements can take place even when the bottom of the drillbit is in hard contact with the bedrock. This autonomous approach to drill management has significant heritage (Worrall et al., 2018).

Nonetheless, the subglacial environment will be challenging. This means that the weight-on-bit control system may be supported by constant monitoring of downhole conditions to ensure that melt-and-refreeze problems are avoided (Timoney et al., 2018). As shown in Fig. 9, these can result in either glazing of the surfaces, or complete freeze-in of the drillbit. The adhesive strength of ice on steel approaches 2 MPa, so either problem is likely to be unrecoverable.

A sensor suite to monitor downhole conditions has been developed and demonstrated within the P-RAID breadboard. The tip of a drillbit, just behind the cutting teeth, has been equipped with an electrode pair and a thermocouple pair. These sensors are wired through the coring bit sidewall, using EDM channels approximately 1 mm in diameter, which extend the full height of the bit itself. The signals are then passed through a slipring, to the controllers.

Melt conditions are detectable by a reduction in downhole resistance, usually from fully open-circuit conditions to readings on the order of 100 kΩ, and by rising temperatures. However, the electrical method may be more valuable due to the possibility of salt depressing the melting point. Examples of electrical and temperature control are shown in Fig. 10.

The upper plot of Fig. 10 shows a campaign where progress in ice-bonded sand is managed using electrical control. The drill progresses from $t = 20$s but, at $t = 50$s, a rise in the measured drilling power correlates with a decrease in downhole resistance. As the resistance falls below a trigger point at $t = 65$ s, the drillbit is withdrawn while the hole re-freezes. A second cycle is then attempted, which penetrates to a slightly greater depth before the process repeats.

The lower plot of Fig. 10 shows a similar campaign in ice-bonded sand, this time managed using temperature control. The withdraw-and-pause manoeuvre is carried out when melt conditions are indicated by downhole temperatures rising above 0 °C and, as before, a slightly greater depth is attained with every cycle.

These demonstrations are important for the future flexibility of the P-RAID system, and the techniques have resulted in drill campaigns to over 170 mm in ice-bonded sand. These depths have not been reached using the weight-on-bit technique, where freeze-in almost always occurs before 100 mm. However, for the remainder of the testing the weight-on-bit method is used so that the difficulties of working in a cold chamber are avoided.

6. P-RAID breadboard testing

6.1. Target materials

In order to establish the performance of the breadboard, a series of laboratory tests are performed on various rock types including: limestone, sandstone and microgabbro. Although these do not necessarily represent the subglacial terrain, the various properties do test specific hardware elements and system operations.

The low strength limestone is easily penetrated, but a combination of rapid progress and chalky fines can lead to auger choking. These tests provide a baseline for the maximum penetration rate, which is then factored into the design of the control algorithm by limiting the size and permissible frequency of progression increments. In addition, the low abrasiveness reduces the wear on the cutting teeth, so it is a useful learning material for other purposes.

Medium strength sandstone provides a more challenging penetration test, but the free-flowing fines are unlikely to clog the auger. The high quartz content rapidly blunts the teeth, such that more than 400 mm to 500 mm of progress becomes difficult without replacements. This allows the performance of the drill system to be characterised over time, in a form of 'accelerated wear' testing.

High strength microgabbro and basalt are best used to test the percussive actuator, which can be operated at elevated power settings that would otherwise choke the auger with limestone cuttings. These rock types are also useful to test the resilience of the teeth and the silver solder used to bond them into the drillbit crowns. As with sandstone, regular tooth replacement is required.

6.2. Performance testing

Fig. 11 details a campaign in limestone. The drillbit had a 40 mm outer diameter and a 25 mm core diameter. Exchangeable drillbit

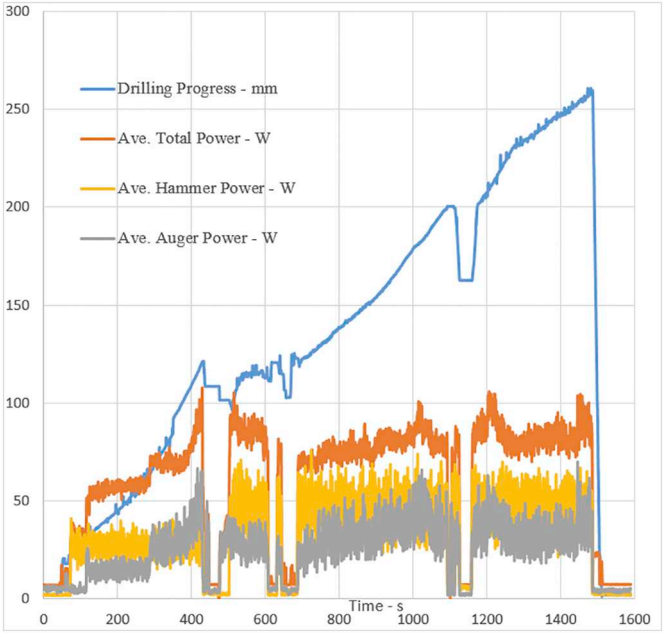

Fig. 11. Drilling data from a successful run in a Hartham Park limestone sample.

Fig. 12. Core samples obtained from tests in Hartham Park limestone (white cores), Locharbriggs sandstone (reddish cores) and microgabbro (grey core).

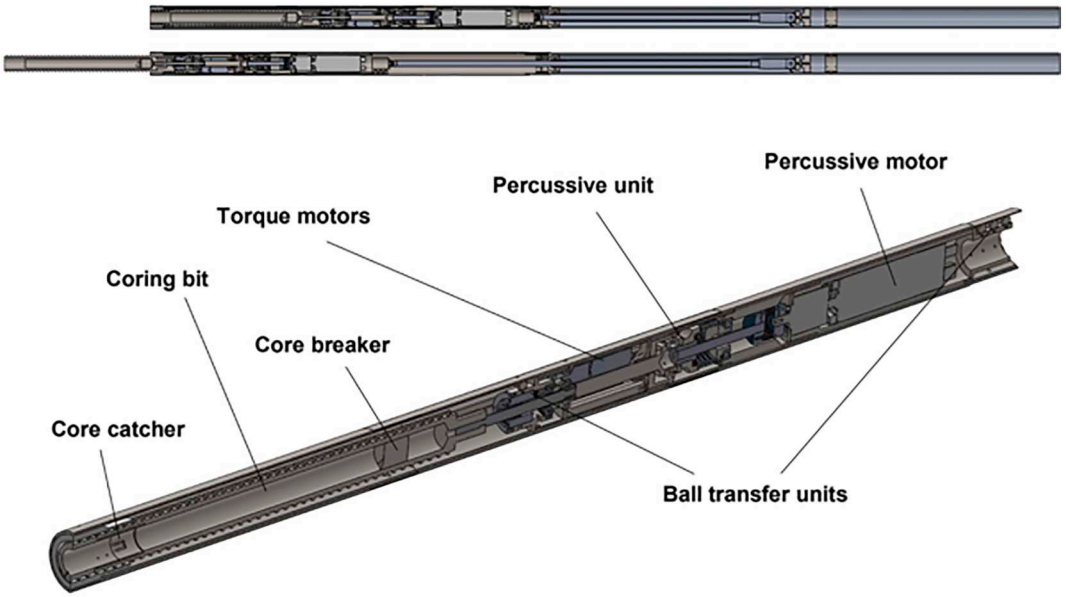

Fig. 13. The P-RAID unit in stowed (top) and full drill extension (below) configurations. Note that the entire stack is around 3.5 m long, and would be mounted below the RAID itself. At bottom, a close-up of the travelling module inside the deployment barrel. The auger exists around the outside of the deployable coring bit.

crowns facilitate continuous testing, and each crown carries two carbide teeth at zero rake angle.

Repeated runs suggest that specific energies of around 300 MJ/m^3, 500 MJ/m^3, and 1800 MJ/m^3 are achievable in limestone, sandstone and microgabbro. Rates-of-progress of around 1800 mm/h, 1100 mm/h, and 300 mm/h, respectively, were noted. Although comparisons for microgabbro are unavailable, the performance obtained in limestone and sandstone is broadly comparable to the literature (Zacny et al., 2008b). Core quality was variable, and Fig. 12 shows examples of limestone, sandstone, and microgabbro sampling.

7. Deployable P-RAID

7.1. Final form factor

The P-RAID breadboard is rearranged into a deployable form factor. Although the key systems were already prototyped within the 80 mm constraint, the linear actuator and downhole electronics, such as motor drivers and power converters, must be reformatted to fit the constraints. The resulting rock sampler is approximately 3.5 m tall, before it is mated with the retained upper section of the RAID drill system to provide an anti-torque stage.

Fig. 13 shows the layout. The upper 1 m of the drill system is given over to the electronics, and terminates with a bulkhead that contains the force transducer. Below the force transducer another 1 m is given over to the linear actuator, which can push the reformatted breadboard module assembly vertically downwards inside the casing, driving the drillbit out of the bottom of the drill system and into the bedrock.

There are some further modifications from the prototype system: without the option of an external guide rail, the travelling module is instead equipped with ball transfer units which track along EDM grooves inside the casing providing the forward linear motion is kept inline; a core-catcher is installed behind the crown to ensure that the rock samples can be extracted; the drillbit is stabilized with a Teflon guide at the bottom of the drill system; and three spikes (not shown in the figure) ensure that the drill system will come to rest just above the bedrock.

However, the operating procedure is now clear. The entire drill system is lowered to the bottom of the borehole, where the anti-torque stage takes hold; the rock sampler deploys the drillbit into the bedrock under local, autonomous control; and then the entire system is withdrawn back to the surface.

7.2. Shakedown testing

As the components were all cold-tested in the breadboard format, the drill system was simply stood up and tested in an ambient laboratory, demonstrating effective and autonomous coring performance in both limestone and sandstone. The system was then shipped to Skytrain Ice Rise, where it was successfully integrated, as shown in Fig. 14, with the RAID anti-torque section, and tested again. However, at this point the auger motors were found to be inoperative, which was unexpected given their previous performance in extended cold test. This problem was not recovered in the field, and is suspected to be related to condensation within the motors jamming the mechanisms or the performance of the motor lubricant in a cold and dry environment.

To address this situation, the motors have now been replaced with an otherwise-identical component qualified to an aerospace standard.

8. Conclusions

This paper presents the developments made by the University of Glasgow, in collaboration with the British Antarctic Survey and Durham University, in the design and initial testing of a subglacial sample retrieval system called P-RAID. This device is capable of extracting 25 mm core samples of limestone, sandstone and microgabbro, of up to 300 mm in length, utilising a rotary-percussive drilling technique, at rates of progress of 1800, 1100 and 300 mm/h in each material. The specific energy of the system is comparable to other drill systems in the literature.

The drill system has been deployed to the polar regions on a shakedown test where it was successfully integrated with the field support equipment, including the winch and the upper section of the RAID. Unexpected issues with the auger motors were identified, but a resolution has been put in place in a laboratory setting.

The system is now considered to be ready to work-up for a deployment, as an initial payload of opportunity, on a science-led campaign where access to the bedrock will be available. Going forwards, it is anticipated that more extensive deployments will facilitate the work of the paleoclimate community across the continent.

Fig. 14. The sonde during setup at Skytrain Ice Rise. The rock sampler is fully extended, showing the teeth, the crown (note the slight discolouration due to frequent silver soldering of the teeth) and the Teflon guide. A large sabot has been fitted to the bottom of the drill system because the ice borehole available at this site was of a larger diameter than would usually be drilled by the RAID device. Inset left: a crown removed from the drillbit, showing the EDM channels for downhole instruments. Inset right: fitting a core catcher behind the crown, which will be secured via the two grub screw positions.

Declaration of Competing Interest

The authors declare that they have no known competing financial interests or personal relationships that could have appeared to influence the work reported in this paper.

Acknowledgements

This research was supported by the Natural Environment Research Council (NE/P003761/1), the UK Space Agency (ST/R00269X/1), the University of Glasgow Impact Acceleration Account, and the British Antarctic Survey through the Collaborative Antarctic Science Scheme.

References

Bar Cohen, Y., Bao, X., Chang, Z., Sherrit, S., 2003. An ultrasonic sampler and sensor platform for in-situ astrobiological exploration. Smart Struct. Mater. 2003.
Cao, P., Yang, C., Zheng, Z., et al., 2014. Low-load diamond drill bits for subglacial bedrock sampling. Ana. Glacio 55 (68), 124–130.
Chu, P., Wilson, J., Davis, K., Shiraishi, L., Burke, K., 2008. Icy soil acquisition device for the 2007 phoenix mars lander. In: NASA Marshall Space Flight Center (Ed.), 39th Aerospace Mechanisms Symposium.
Chu, P., Spring, J., Zacny, K., 2014. ROPEC - ROtary PErcussive coring drill for mars sample return. In: 42nd Aerospace Mechanisms Symposium. NASA Goddard Space Flight Center.
Church, A., 2013. Sea level change. In: Climate Change 2013: The Physical Science Basis. Contribution of Working Group I to the Fifth Assessment Report of the Intergovernmental Panel on Climate Change. Cambridge University Press, Cambridge, UK and New York, NY, USA.
Clow, G.D., Koci, B., 2002. A fast mechanical-access drill for polar glaciology, paleoclimatology, geology, tectonics and biology. Mem. Natl. Inst. Polar Res. 56, 1–30 Spec Issue.
Dutton, A., Carlson, A.E., Long, A.J., Milne, G.A., et al., 2015. Sea-level rise due to polar ice-sheet mass loss during past warm periods. Science 349, 153.
Flowerdew, M.J., Tyrrell, S., Riley, T.R., Whitehouse, M.J., et al., 2012. Distinguishing East and West Antarctic sediment sources using the Pb isotope composition of detrital K-feldspar. Chem. Geol. 292–293, 88–102.
Fretwell, P., Pritchard, H.D., Vaughan, D.G., Bamber, J.L., Barrand, N.E., et al., 2013. Bedmap2: improved ice bed, surface and thickness datasets for Antarctica. Cryosphere 7, 375–393.
Goodge, J.W., Severinghaus, J.P., 2016. Rapid Access Ice Drill: a new tool for exploration

of the deep Antarctic ice sheets and subglacial geology. J. Glaciol. 1–6.
Han, G., Dusseault, M., 2005. Dynamically modelling rock failure in percussion drilling. In: The 40th U.S. Symposium on Rock Mechanics, Alaska Rock, AL, USA.
IDDO, 2015. Agile sub-ice geological drill system design review. U.S. Ice Drilling Program.
IPICS, 2020. White Paper, "Ice Core Drilling Technical Challenges". Undated. .
Melamed, Y., Kiselev, A., Gelfgat, M., Dreesen, D., Blacic, J., 2000. Hydraulic hammer drilling technology: developments and capabilities. J. Energy Resour. Technol. 122 (1), 1–8.
Mulvaney, R., Bremner, S., Tait, A., Audley, N., 2002. A medium-depth ice core drill. In: Fifth International Workshop on Ice Drilling Technologies, Tokyo, Japan.
Mulvaney, R., Alemany, O., Possneti, P., 2014a. The Berkner Island (Antarctica) ice-core drilling project. Ana. Glacio 55 (68).
Mulvaney, R., Triest, K., Alemany, O., 2014b. The James Ross island and the fletcher promontory ice core drilling projects. Ana. Glacio 55 (68).
National Reseach Council, 2011. Future Scientific Opportunities in Antarctica and the Southern Ocean. National Academies Press, Washinton DC, USA.
Norton, R.L., 2009. Cam design and manufacturing handbook. Industrial Press, New York, NY, USA.
Okon, A., 2010. Mars science laboratory drill. In: NASA Kennedy Space Center (Ed.), 40th Aerospace Mechanisms Symposium.
Orosei, M., Lauro, S.E., Pettinelli, E., Cicchetti, A., Coradini, M., et al., 03 Aug 2018. Radar evidence of subglacial liquid water on mars. Science 361 (6401), 490–493. https://doi.org/10.1126/science.aar7268.
Quan, Q., et al., 2012. Development of a rotary-percussive drilling mechanism (RPDM). In: IEEE International Conference on Robotics and Biomimetics, Guangzhou, China.
Rix, J., Mulvaney, R., Hong, J., Ashurst, D., April 2019. Development of the British antarctic survey rapid access isotope drill. J. Glaciol. 65 (250), 288–298 (in press).
Samuel, G. Robello, 1996. Percussion drilling – is it a lost technique? A review. In: Permian Basin Oil and Gas Recovery Conference, Midland, TX, USA.
Spector, P., Stone, J., Pollard, D., Hillebrand, T., Lewis, C., Gombiner, J., 2018. West Antarctic sites for subglacial drilling to test for past ice-sheet collapse. Cryosphere 12, 2741–2757.
Sugden, D.E., Bentley, M.J., Cofaigh, C.O., 2012. Geological and geomorphological insights into Antarctic ice sheet evolution. Phil. Trans. R. Soc. A 364, 1607–1625.
Talalay, P.G., 2013. Subglacial till and bedrock drilling. Cold Reg. Sci. Technol. 86, 142–166.
Timoney, R., Worrall, K., Firstbrook, D., Harkness, P., 2018. The development of a heuristic thermal control system for the ultrasonic planetary core drill. In: ASCE Earth and Space 2018, Cleveland, OH, USA.
Triest, J., Mulvaney, R., Alemany, O., 2014. Technical innovations and optimization for intermediate ice-core drilling operations. Ana. Glacio. 55 (68), 243–252.
Wang, J., Cao, P., Liu, C., Talalay, P.G., 2015. Comparison and analysis of subglacial bedrock core drilling technology in Polar Regions. Polar Sci. 9, 208–220.
Worrall, K., Timoney, R., Harkness, P., Li, X., Lucas, M., 2018. UPCD: field trial results and further work. In: ASCE Earth and Space 2018, Cleveland, OH, USA.
Zacny, K., Cooper, G.A., 2007. Methods for cuttings removal from holes drilled on mars. Int. J. Mars Sci. Explor. 3, 42–56.
Zacny, K., Quayle, M., Cooper, G., 2005. Enhancing cuttings removal with gas blasts while drilling on Mars. J. Geophys. Res. 3 (110), 42–56.
Zacny, K., Bar-Cohen, Y., Brennan, M., Briggs, G., Cooper, G., Davis, K., et al., 2008a. Drilling systems for extraterrestrial subsurface exploration. Astrobiology 8 (3), 665–706.
Zacny, K., Bar-Cohen, Y., Brennan, M., Briggs, G., Cooper, G., et al., 2008b. Drillings systems for extraterrestrial subsurface exploration. Astrobiology 8 (3), 665–706.
Zacny, K., et al., 2013. Reaching 1m deep on Mars: the icebreaker drill. Astrobiology 13 (12), 1166–1198.